


Translocator Protein (TSPO) Alleviates Neuropathic Pain by Activating Spinal Autophagy and Nuclear SIRT1/PGC-1 α Signaling in a Rat L5 SNL Model

Can Hao*, Bingjie Ma , Nan Gao, Tian Jin, Xiaoming Liu 

Pain Management Center, Shanghai Xinhua Hospital, School of Medicine, Shanghai Jiaotong University, Shanghai, 210092, People's Republic of China

*These authors contributed equally to this work

Correspondence: Xiaoming Liu, Pain Management Center, Shanghai Xinhua Hospital, School of Medicine, Shanghai Jiaotong University, 1665# Kongjiang Road, Shanghai, 210092, People's Republic of China, Tel +86-17721213706, Fax +86-21-25078707, Email brightlxm@gmail.com

Purpose: Recent studies showed promotion of astrocyte autophagy in the spinal cord would provide analgesic effects. Silent information regulator T1 (SIRT1) and α subunit of peroxisome proliferator-activated receptor- γ coactivator-1 (PGC-1 α) are two master regulators of endogenous antioxidant defense and mitochondrial biogenesis. They play vital roles in both autophagy and neuropathic pain (NP). Our previous study showed that TSPO agonist Ro5-4864 elicited potent analgesic effects against NP, but the mechanisms remain unclear. This study aims to investigate the effects of TSPO agonist Ro5-4864 on autophagy and nuclear SIRT1/PGC-1 α signaling in spinal dorsal horn.

Methods: A rat model of L5 spinal nerve ligation (SNL) was adopted. Rats were randomly assigned to the Sham group, the SNL group, the Ro (TSPO agonist Ro5-4864) group and the Ro+3-MA group. The behavior assessments were conducted at baseline, on Day 1, 3, 7 and 14 after SNL. The autophagy-related proteins (ATG7, Beclin1, LC3, and P62) in spinal dorsal horn were assayed and the nuclear SIRT1/PGC-1 α and downstream factors were analyzed.

Results: Ro5-4864 alleviated the mechanical allodynia induced by SNL ($P < 0.01$ vs the SNL group), which could be totally abrogated by autophagy inhibitor 3-MA ($P < 0.01$ vs the Ro group). SNL induced elevated ATG7 ($P < 0.01$), Beclin1 ($P < 0.01$) and LC3-II/LC3-I ($P < 0.01$) contents and P62 accumulation ($P < 0.01$) on Day 7 and Day 14, which suggested an autophagy flux impairment. Ro5-4864 augmented ATG7 ($P < 0.01$), Beclin1 ($P < 0.01$) and LC3-II/LC3-I ($P < 0.05$) with decreased P62 ($P < 0.01$), which indicated a more fluent autophagic process. These effects were also totally abrogated by 3-MA ($P < 0.01$). Furthermore, Ro5-4864 activated the spinal nuclear SIRT1/PGC-1 α signaling pathway.

Conclusion: TSPO improved both autophagy impairment and mitochondrial biogenesis, which may provide a new strategy for the treatment of NP.

Keywords: translocator protein, TSPO, neuropathic pain, autophagy, silent information regulator T1, SIRT1, α subunit of peroxisome proliferator-activated receptor- γ coactivator-1, PGC-1 α

Introduction

Autophagy is believed as a stress adaptation and offers an alternative cell death pathway.¹ Previous studies about autophagy and autophagy-related genes (ATG) mainly focused on tumor cells. Some ATGs dysfunction may correlate with tumor progression and poorer patient survival.² Recently, researchers have paid more attention to the role of autophagy in the nervous system. Scientists reported that autophagic dysfunction is associated with neurodegenerative diseases such as Huntington's disease³ and spinocerebellar ataxia,⁴ which are associated with ineffective lysosomal clearance by autophagy. Moreover, autophagic dysfunction played a crucial role in nerve injury and neuropathic pain.⁵

Recently, Li et al reported that activation of autophagy relieved pain during both neuropathic pain (NP) induction and maintenance.⁶ Several studies found that autophagic activity was disrupted in both spinal neurons and glial cells in NP.^{5,6} Li et al found that the autophagy impairment was mainly located in spinal cord astrocytes during the maintenance phase of NP.⁶ Jin et al provided the direct evidence that the promotion of astrocyte autophagy would provide analgesic effects in both the spinal cord and in vitro primary cultured astrocytes.⁷

α subunit of peroxisome proliferator-activated receptor- γ coactivator-1 (PGC-1 α) was the first member identified as a cofactor for the nuclear hormone receptor PPAR γ that is required for the adaptive thermogenic response to lower temperatures. It also plays a vital role in autophagy and mitophagy according to the cellular metabolic state.^{8,9} Silent information regulator T1 (SIRT1) is known as the only protein that is able to deacetylate and activate PGC-1 α .¹⁰ Recent studies reported that PGC-1 α signaling regulates detoxifying astrocyte responses to hypoxic and oxidative stresses, which implicated this signaling as an important regulator of astrocyte reactivity.^{11,12}

The translocator protein (18 kDa) (TSPO) is a small molecular weight protein which is localized in the outer mitochondrial membrane. It is expressed primarily in steroid-synthesizing tissues, including the nervous system.¹³ Our previous study showed that TSPO agonist Ro5-4864 or recombinant lentivirus over-expressing of TSPO RNA could both elicit potent analgesic effects against neuropathic pain, which was attributed to inhibition of spinal astrocytes activation and astrocyte-to-neuron signaling.¹⁴ Meanwhile, TSPO was verified to play an important role in regulating mitochondrial function and mitophagy.^{15,16} Whether TSPO agonist can affect astrocyte autophagy in spinal DH, and whether it would modulate the SIRT1/PGC-1 α signaling have not been reported yet. This paper therefore aims to 1) verify the astrocyte autophagy in spinal DH after rat L5 spinal nerve ligation (SNL) model; 2) study the effects of TSPO on autophagy-related proteins in vivo; 3) explore the effects of TSPO ligands on SIRT1/PGC-1 α signaling in vivo.

Materials and Methods

Animals and Drugs

The following experimental protocol was approved by Animal Care and Use Committee in Shanghai Xinhua Hospital (Approval No. XHEC-F-2021-009). All procedures were performed in accordance with the Guide for the Care and Use of Laboratory Animals of the International Association for the Study of Pain. All the male Sprague-Dawley rats (body weight, 200 \pm 20g, purchased from the Animal Center of the Chinese Academy of Science in Shanghai) were acclimated in a quarantine room at the animal center in Shanghai Xinhua Hospital for five days before surgery.

Ro5-4864((7-chloro-5-(4-chlorophenyl)-1,3-dihydro-1-methyl-2H-1,4-benzodiazepine-2)), autophagy inhibitor 3-Methyladenine (3-MA) were both dissolved in dimethyl sulfoxide (DMSO, 8.72%), which were all purchased from Sigma Aldrich (St. Louis, MO, USA). TSPO agonist Ro5-4864 was injected intrathecally (0.2 μ g/ μ l \times 10 μ l). Animals in vehicle group and sham group received the same volume of 8.72%DMSO (10 μ L).

Experimental Protocol

A total of 120 rats were randomly assigned to four experimental groups (n = 30 in each group): (1) the sham group (Sham group); (2) the vehicle (control) group (SNL group); (3) the Ro group (2 μ g/10 μ l Ro5-4864, i.t. repeated for 3 days, on Day 3–5); (4) the Ro + 3-MA group (2 μ g/10 μ l Ro5-4864+4 μ g/10 μ l 3-MA, i.t. repeated for 3 days, on Day 3–5). Behavioral assessments were performed in all animals before surgery (day 0) and on Day 1, 3, 7 and 14 after SNL surgery or sham operation, separately. The ipsilateral L5 spinal cords were collected at baseline, Day 7, and Day 14 (n = 10 for each point of time in every group, among these 10 rats, 3 killed for immunofluorescence, 4 for Western blot, and 3 for electromicroscopic assessment). The scheme of protocol is shown in Figure 1.

Surgical Procedures

Neuropathic pain was induced using the methods of our previous study.¹⁴ Briefly, after rats were anesthetized (50 mg/kg sodium pentobarbital, ip), they were placed in a prone position. A midline incision was made and the paraspinal muscles were separated to expose the left L5 spinal nerves. Then the L5 nerve was tightly ligated with a 3-0 silk thread without

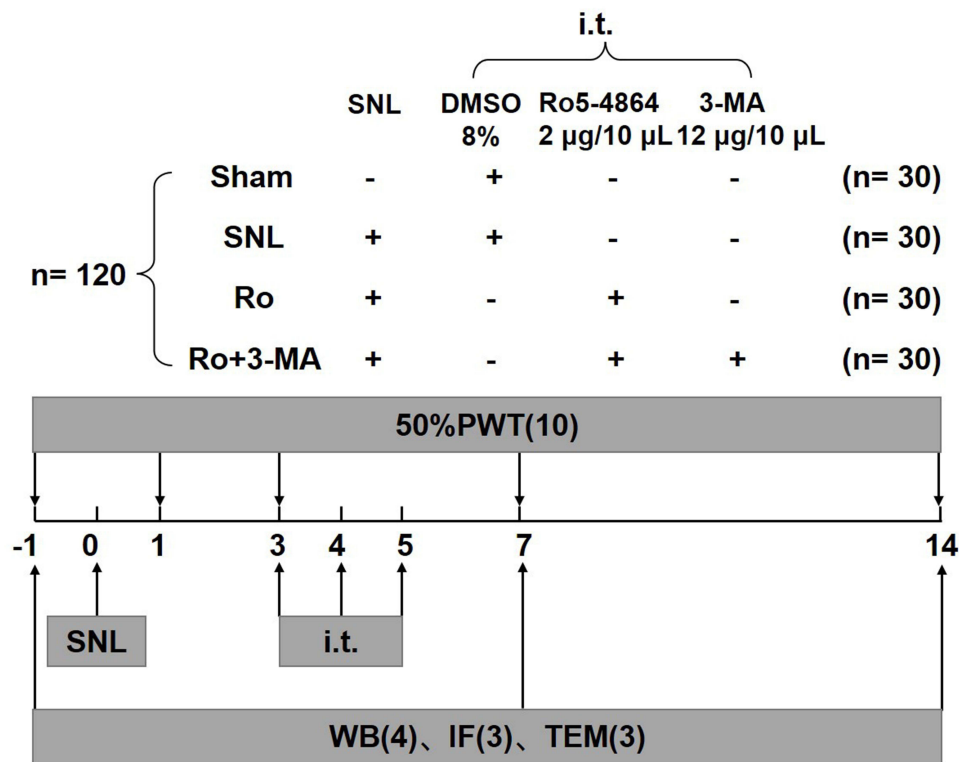


Figure 1 The scheme of experiment protocol. A total of 120 rats were randomly assigned to four experimental groups ($n = 30$ in each group): (1) the sham group (Sham group); (2) the vehicle (control) group (SNL group); (3) the Ro group ($2\mu\text{g}/10\mu\text{l}$ Ro5-4864, i.t. repeated for 3 days, on Day 3–5); (4) the Ro + 3-MA group ($2\mu\text{g}/10\mu\text{l}$ Ro5-4864+ $4\mu\text{g}/10\mu\text{l}$ 3-MA, i.t. repeated for 3 days, on Day 3–5). Behavioral assessments were performed in all animals before surgery (day 0) and on Day 1, 3, 7 and 14 after SNL surgery or sham operation, separately. The ipsilateral L5 spinal cords were collected at baseline, Day 7, and Day 14 ($n = 10$ for each point of time in each group, among these 10 rats, 3 killed for immunofluorescence, 4 for Western blot, and 3 for electromicroscopic assessment).

damage to the dorsal root ganglion or other nerves. The wound was finally irrigated with saline solution and closed after surgical procedure.

Behavioral Assessment

The day of surgical procedure was named as Day 1. Behavioral assessments were performed before surgery (Day 0, or baseline) and on test days after sham operation or SNL surgery using the methods of our previous study.¹⁴ Each rat was placed in the testing chamber and allowed to acclimate for 30 minutes before testing. The withdrawal thresholds were determined according to the “up–down method” by standard Von Frey filaments (Stoelting Co, Wood Dale, IL). According to the response pattern described by Chaplan et al,¹⁷ we calculated and recorded the 50% response threshold. The minimum score was 0.25 g, and the maximum score was 26 g. All behavioral tests were assessed by the same author (Hao C) who is not aware of the group assignment.

Immunofluorescence

Rats were anesthetized and perfused with 300 mL of 0.9% saline and 250 mL of 4% paraformaldehyde separately. We selected the L5 spinal segments. After post-fixed overnight at 4°C, the samples were immersed in 30% sucrose in 0.1 M phosphate-buffered saline (PBS) at 4°C. Using the cryostat (LEICA CM1900 UV), the spinal cord sections were cut transversely at 30 µm thick. The following immunofluorescence examinations were performed as in our previous study.¹⁴ The primary antibodies used were as follows: LC3: 1:200, rabbit, Cell Signaling Technology; TSPO: 1:100, rabbit, LifeSpan BioSciences. A Leica laser scanning confocal microscope (Leica TCS SP5 II) was used to acquire images. A computer software (Leica AF Version 2.3.0) was used to analyze and compare the fluorescent intensity. The magnification of figures are $\times 50$ or $\times 400$, as indicated in figure legends. For LC3 fluorescent intensity comparison, 3 sections from the L5 spinal cord segments were randomly selected

in every animal ($n = 3$ on Day 7 and Day 14 separately). An image in a rectangle on the superficial dorsal horn (laminae I–III) was captured with a numerical intensity value and was calculated with a computer-assisted imaging analysis system (Image J). The intensity of the background was subtracted in each section.

Transmission Electron Microscopy (TEM)

Adult male SD rats were anesthetized, as described above. The ipsilateral spinal DH was quickly harvested within 1–3 minutes. The size of tissue block sample was about 1 mm^3 . Samples were transferred with fresh TEM fixative into an EP tube, and then samples were fixed at 4°C for preservation. After washing by 0.1 M PB ($\text{pH} = 7.4$), the tissue blocks were post-fixed with 1% OsO_4 in 0.1 M PB ($\text{pH} = 7.4$) for 2h at room temperature, dehydrated through a graded series of ethanol and acetone, resin permeated and embedded. The embedding models with resin and samples were moved into 65°C oven to polymerize for more than 48h. The resin blocks were cut to 60–80 nm thin on the ultramicrotome (Leica UC7; Leica, Vienna, Austria), and the tissues were fished out onto the 150 meshes cuprum grids with formvar film. With 2% uranium acetate saturated alcohol solution avoiding light staining for 8 min, samples were rinsed in 70% ethanol 3 times and then rinsed in ultra pure water 3 times. With 2.6% Lead citrate avoiding CO_2 staining for 8 min, samples were then rinsed with ultra pure water 3 times. After dried by the filter paper, the cuprum grids were put into the grids board and dried overnight at room temperature. Finally, the cuprum grids were observed under TEM (HT7800, Hitachi, Tokyo, Japan) and images were taken. For TEM quantitative assessment, 3 views from every sample were randomly selected ($n = 3$ in every group on Day 14).

Western Blot Analysis

The ipsilateral spinal cord was collected. Using BCA Protein Assay Kit (Pierce Biotechnology, Rockford, IL, USA), every sample was quantified of its protein content. A total of $20\text{ }\mu\text{g}$ protein were loaded for each lane and separated on 10% or 12.5% SDS-PAGE gel and then transferred to $0.4\text{ }\mu\text{m}$ PVDF membranes. The blots were incubated overnight at 4°C with the following primary antibodies (ATG7: 1:1000, rabbit, Cell Signaling Technology; LC3: 1:1000, rabbit, Cell Signaling Technology; Beclin1: 1:1000, rabbit, Cell Signaling Technology; P62: 1:1000, rabbit, Cell Signaling Technology; actin: 1:1000, rabbit, Cell Signaling Technology; PGC-1 α : 1:1000, goat, Abcam; SIRT1: 1:1000, rabbit, Abcam; Nrf2: 1:1000, rabbit, Cell Signaling Technology; HO-1: 1:1000, rabbit, Cell Signaling Technology), then incubated with a goat anti-rabbit or anti-mouse HRP-conjugated secondary antibody (Anti-Rabbit: 1:1000, Beyotime; Anti-Goat: 1:5000, YEASEN). Protein signals were detected using an enhanced chemiluminescence (ECL) detection system (Pierce Biotechnology, Rockford, IL, USA). An anti- β -actin antibody (1:1000, Cell Signaling Technology, USA) or an anti-laminA/C antibody (1:10000, ABClonal, China) was used to normalize sample loading and transfer. The intensity of the selected bands was analyzed using Image J software (National Institutes of Health [NIH], Bethesda, MD, USA).

Statistical Analysis

Statistical analyses were performed by using SPSS 10.0. Behavioral assessment was first analyzed using a repeated measures two-way analysis of variance followed by Bonferroni post hoc tests. Then, multivariate analysis of variance (ANOVA) was performed followed by Tukey's tests to further compare behavioral assessments among different groups at the same point of time. For fluorescent intensity comparison, TEM quantitative comparison and Western blot analyses, one-way ANOVA were performed followed by the Tukey post hoc test. All data were presented as mean \pm standard deviation (SD). A two-sided $P < 0.05$ was considered significant.

Results

TSPO Agonist Ro5-4864 Alleviated the Neuropathic Pain Induced by SNL, Which Can Be Abrogated by Autophagy Inhibitor 3-MA

SNL induced a significant decrease of the ipsilateral paw 50% withdrawal threshold (PMWT) during the whole period compared with the Sham group. Intrathecal injection of Ro5-4864 at $2\mu\text{g}$ repeated for three days remarkably increased

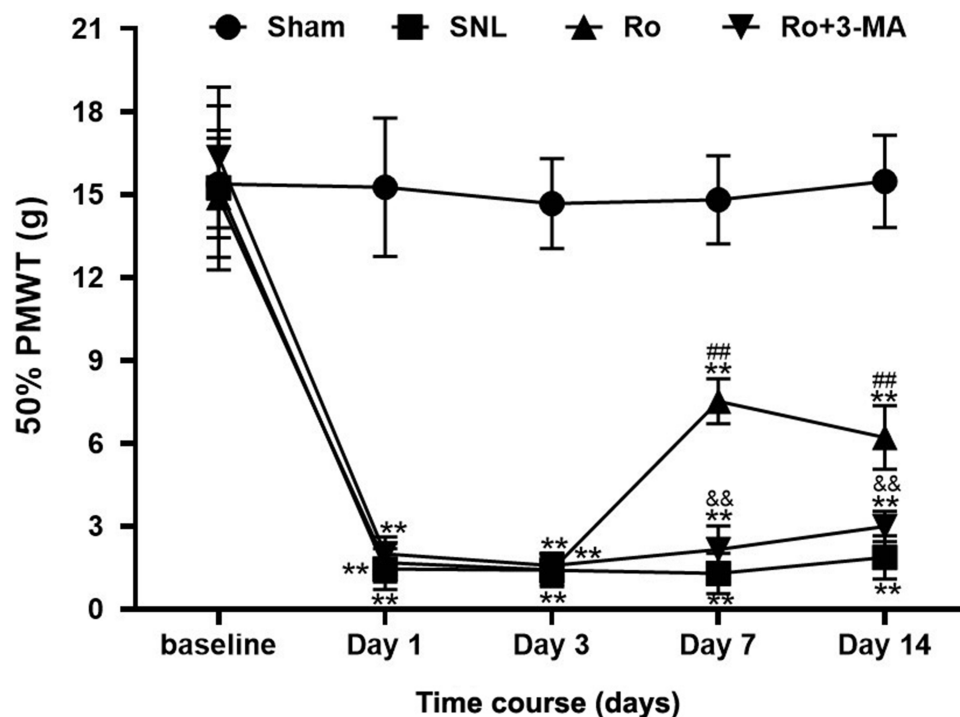


Figure 2 Effects of TSPO agonist Ro5-4864 with or without autophagy inhibitor 3-MA on mechanical allodynia induced by SNL. Behavioral assessments of the four groups. ** $P < 0.01$ compared with the Sham group at the same point in time. ### $P < 0.01$ compared with the SNL (control) group at the same point in time. && $P < 0.01$ compared with the Ro group at the same point in time. $n = 10$ in each group.

the 50% PMWT compared with the SNL group ($P < 0.01$ vs the SNL group, Figure 2). This result is consistent with our previous study. This anti-allodynia effect of Ro5-4864 can be totally abrogated by autophagy inhibitor 3-MA ($P < 0.01$ vs the Ro group, Figure 2). The comparison results of the four groups on Day 7 and Day 14 separately are also shown in Figure 2.

Effects of TSPO Agonist Ro5-4864 on Autophagy-Related Proteins

Microtubule associated protein 1 light chain 3 (LC3) has two forms: LC3-I and LC3-II. LC3-II/LC3-I is a classic marker representing autophagic state. The signals of LC3 after SNL were first examined using immunofluorescence. Representative immunofluorescence pictures of L5 spinal DH are shown in Figure 3A. There was a very low level of basal LC3 signal within the L5 spinal DH at baseline, which was slightly increased on Day 7 (about 1.25-fold) and on Day 14 (about 1.27-fold) following SNL ($P < 0.05$ vs the Sham group, Figure 3B). Ro5-4864 upregulated the signal increase of LC3, which is about 1.52-fold on Day 7 and maintained on Day 14 ($P < 0.05$ vs the Sham group and the SNL group, Figure 3B). This effect could be remarkably inhibited by 3-MA ($P < 0.01$ on Day 7 and $P < 0.05$ on Day 14 vs the Ro group, Figure 3B). Double staining was then performed. The results showed that, compared with the Sham group, the signals that expressed both TSPO and LC3 increased after SNL. Moreover, the signals also augmented in the Ro group versus the SNL group. And 3-MA remarkably abrogated the effects of Ro5-4864 (Figure 3C).

Then Western blots were performed to investigate the contents of some autophagy-related proteins. ATG7 is a typical autophagy-related gene, which regulates ATG5, leading to the conjugation of LC3 to a lipid.¹⁸ Therefore, the spinal DH expressions of ATG7, Beclin1, LC3-II/LC3-I and P62 after SNL were all examined by Western blot. The results showed that, compared with the sham group, the content of ATG7 ($P < 0.01$, Figure 4A and B), Beclin1 ($P < 0.01$, Figure 4A and D), LC3-II/LC3-I ($P < 0.01$, Figure 4A and F) and p62 ($P < 0.01$, Figure 4A and C) significantly increased on Day 7 and Day 14 after SNL. Nevertheless, TSPO agonist Ro5-4864 augmented the activation of ATG7 ($P < 0.01$, Figure 4B), Beclin1 ($P < 0.01$, Figure 4D) and LC3-II/LC3-I ($P < 0.05$, Figure 4F). P62 content in the Ro group showed remarkable

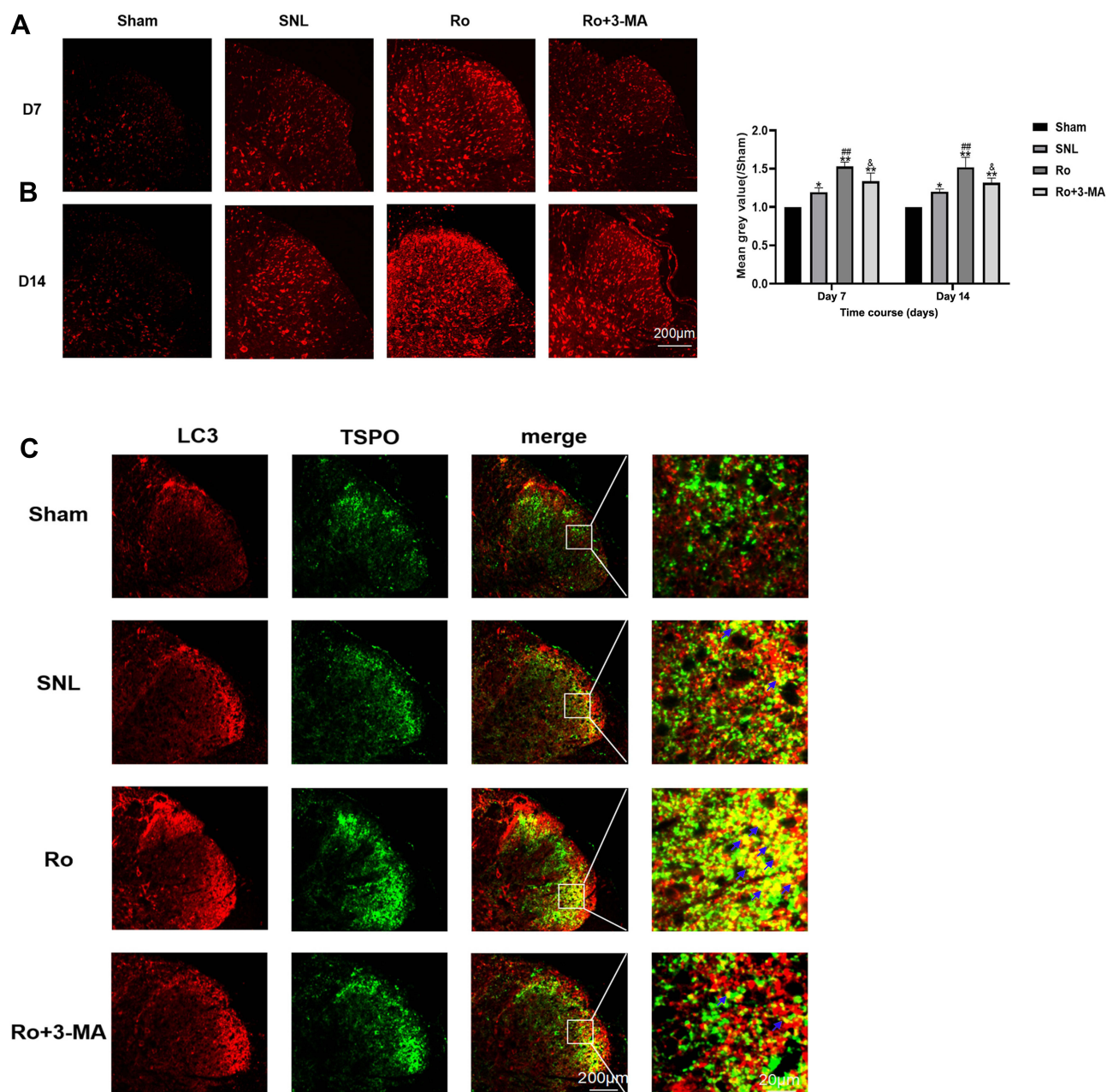


Figure 3 Single and Double staining of LC3 signals in spinal dorsal horn by immunofluorescence. **(A)** Representative immunofluorescent pictures of single staining of LC3 signals in spinal dorsal horn of the four groups on Day 7 and Day 14. **(B)** LC3 signals intensity in the spinal dorsal horn the four groups on Day 7 and Day 14. * $P < 0.05$ and ** $P < 0.01$ compared with the Sham group at the same point in time. *** $P < 0.001$ compared with the SNL (control) group at the same point in time. & $P < 0.05$ compared with the Ro group at the same point in time. **(C)** Representative immunofluorescent pictures of double staining of LC3 and TSPO signals in spinal dorsal horn of the four groups on Day 7 and Day 14.

decrease on Day 7 and Day 14 versus the same point of time in the SNL group ($P < 0.01$, Figure 4C). 3-MA totally abrogated the effects of Ro5-4864 on these autophagic-related proteins ($P < 0.01$, Figure 4C–F).

Effects of Ro5-4864 on Ultrastructure of Spinal DH

To assess the autophagosome-lysosomal machinery, transmission electron microscopy (TEM) was applied to evaluate the number and ultrastructure of autophagosomes, autolysosomes and lysosomes in the cytoplasm of astrocytes in the spinal DH on Day 14. Representative electromicroscopic views of autophagosomes (red arrow), autolysosomes (yellow arrow) and lysosomes (blue arrow) in spinal dorsal horn of the four groups are presented in Figure 5A. There were only a few

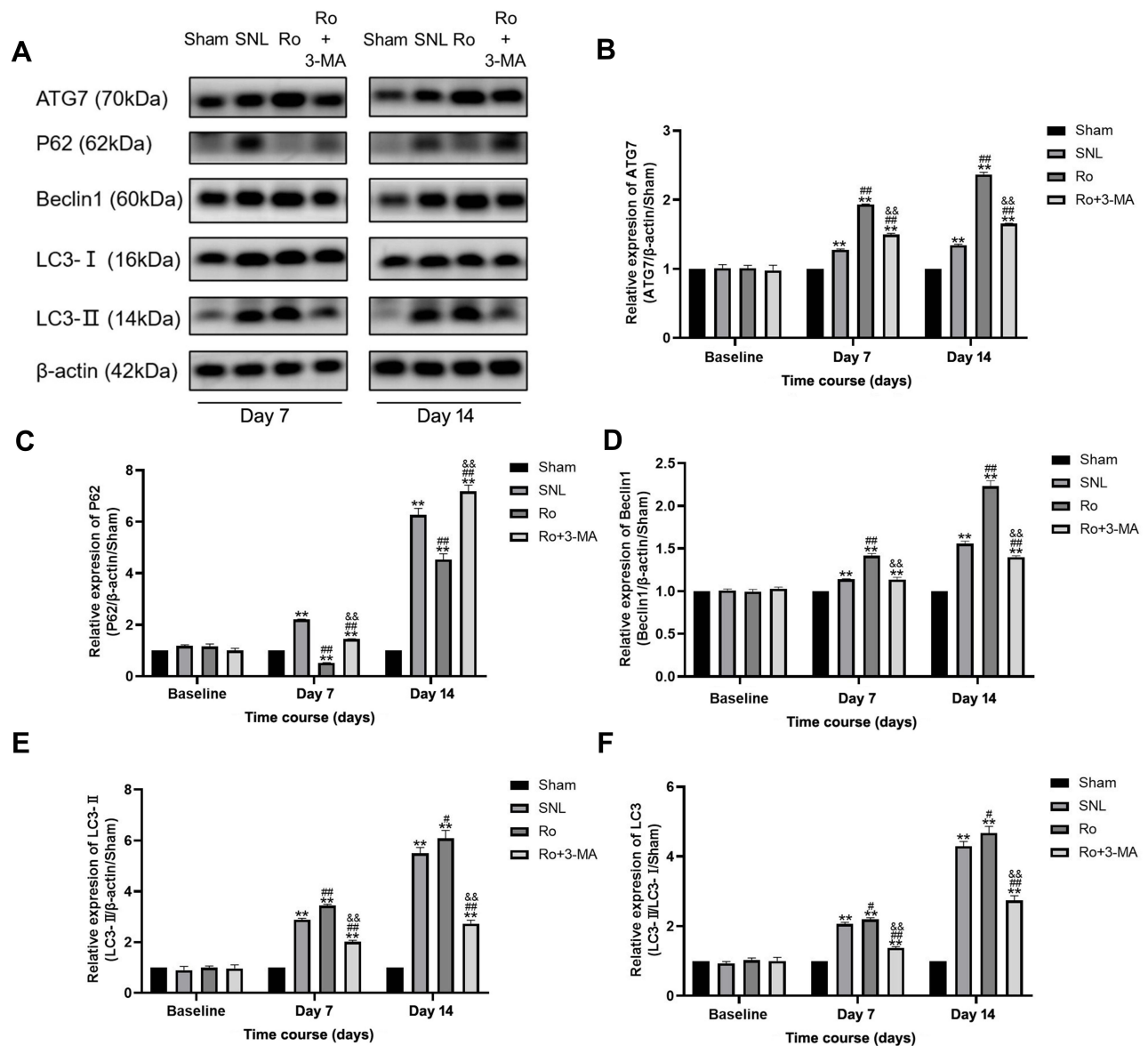


Figure 4 Effects of TSPO agonist Ro5-4864 with or without autophagy inhibitor 3-MA on autophagic proteins. **(A)** Representative immunoblots for ATG7, P62, Beclin I, and LC3-I/LC3-II contents of the four groups on Day 7 and Day 14. **(B–F)** Illustration of the relative expression of ATG7/β-actin/Sham **(B)**, P62/β-actin/Sham **(C)**, Beclin I/β-actin/Sham **(D)**, LC3-II/β-actin/Sham **(E)**, and LC3-II/LC3-I/Sham **(F)** of the four groups. ** $P < 0.01$ compared with the Sham group at the same point in time. # $P < 0.05$ and ### $P < 0.01$ compared with the SNL (control) group at the same point in time. && $P < 0.01$ compared with the Ro group at the same point in time. $n = 4$ for each point of time in each group.

autophagosomes, lysosomes and autolysosomes in the Sham group. The SNL group showed slight elevation of autophagosomes, but fewer lysosomes ($P < 0.05$ vs the Sham group, [Figure 5B](#)) and autolysosomes, which indicated an impaired autophagy. The Ro group showed more autophagosomes ($P < 0.01$ vs the SNL group, [Figure 5B](#)), autolysosomes ($P < 0.01$ vs the SNL group, [Figure 5B](#)) and lysosomes ($P < 0.01$ vs the SNL group, [Figure 5B](#)), which indicated a more activated autophagy and a more fluent autophagy process. This effect of Ro was abrogated by 3-MA ($P < 0.01$ vs the Ro group, [Figure 5B](#)).

Effects of Ro5-4864 on Nuclear SIRT1/PGC-1 α Signaling Pathway

Finally, Western blots were performed to assay the effects of Ro5-4864 on spinal nuclear SIRT1/PGC-1 α and downstream Nrf2 and HO-1 expressions. There was a basal level of SIRT1 and PGC-1 α expressions within the L5 spinal DH at baseline. SIRT1 significantly increased on Day 7 ($P < 0.01$) and on Day 14 ($P < 0.01$) following SNL ([Figure 6A](#) and [B](#)). PGC-1 α also

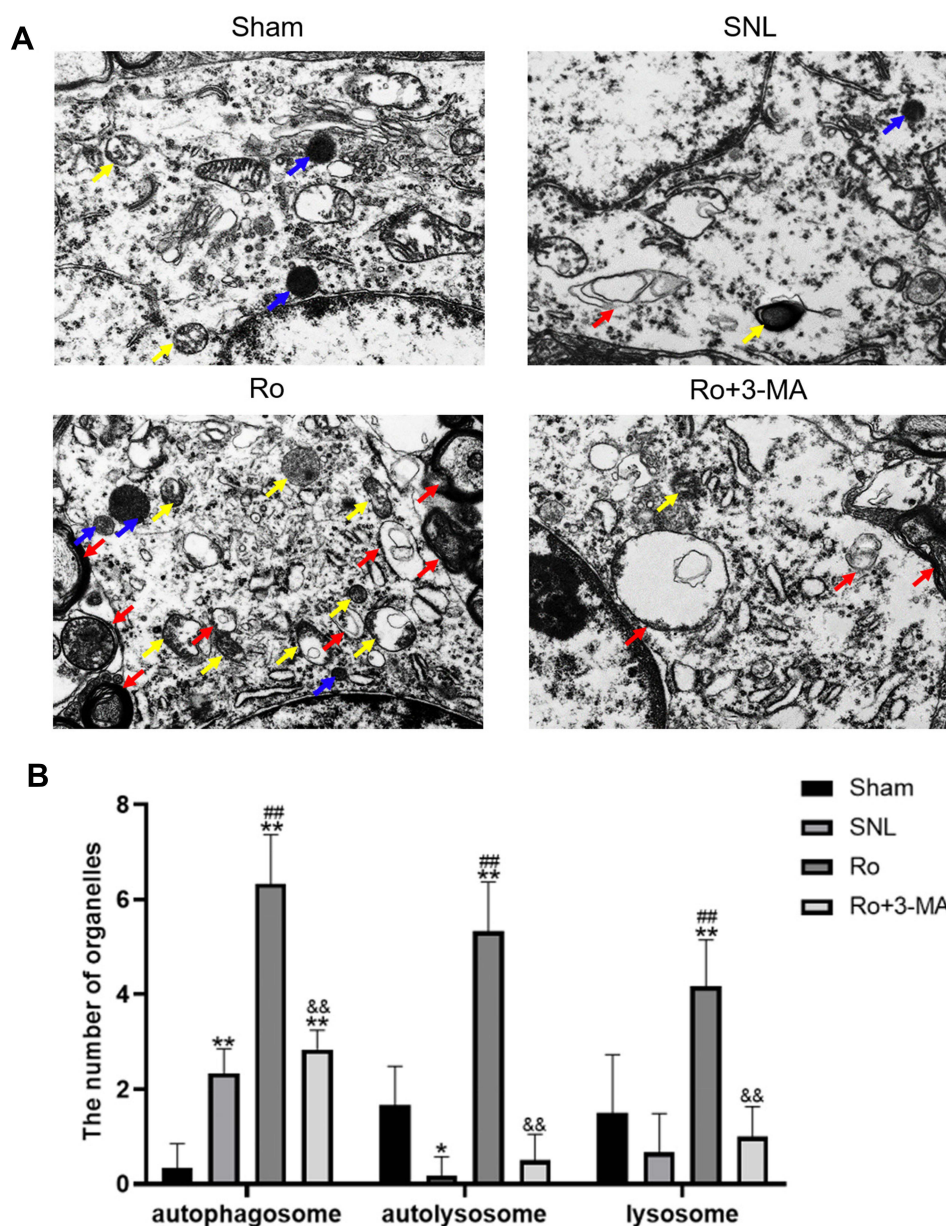


Figure 5 Effects of Ro5-4864 on ultrastructure of spinal dorsal horn by TEM. **(A)** Representative electromicroscopic views of autophagosomes (red arrow), autolysosomes (yellow arrow) and lysosomes (blue arrow) in spinal dorsal horn of the four groups. Magnification, $\times 8,000$ **(B)** Illustration of quantitative score of autophagosomes, autolysosomes and lysosomes on Day 14 of the four groups. * $P < 0.05$ and ** $P < 0.01$ compared with the Sham group. ### $P < 0.01$ compared with the SNL (control) group. && $P < 0.01$ compared with the Ro group.

remarkably elevated on Day 7 ($P < 0.01$) and maintained on Day 14 ($P < 0.01$) (Figure 6A and C). Ro5-4864 provided more activated nuclear SIRT1 and PGC-1 α vs the SNL group ($P < 0.01$ on Day 7 and Day 14, Figure 6A–C). There was a very low level of nuclear Nrf2 contents within the L5 spinal DH at baseline. SNL induced nuclear Nrf2 activation ($P < 0.01$ on Day 7 and Day 14 vs the Sham group), while Ro5-4864 significantly augmented this activation ($P < 0.01$ on Day 7 and Day 14 vs the SNL group, Figure 6A and D). Cytoplasmic HO-1 was also assayed. There was no significant difference in HO-1 expression among the three groups in baseline. SNL activated HO-1 on Day 7 ($P < 0.05$, Figure 6E and F) and Day 14 ($P < 0.01$, Figure 6E and F). Ro5-4864 administration provided more elevated cytoplasmic HO-1 ($P < 0.01$, Figure 6E and F).

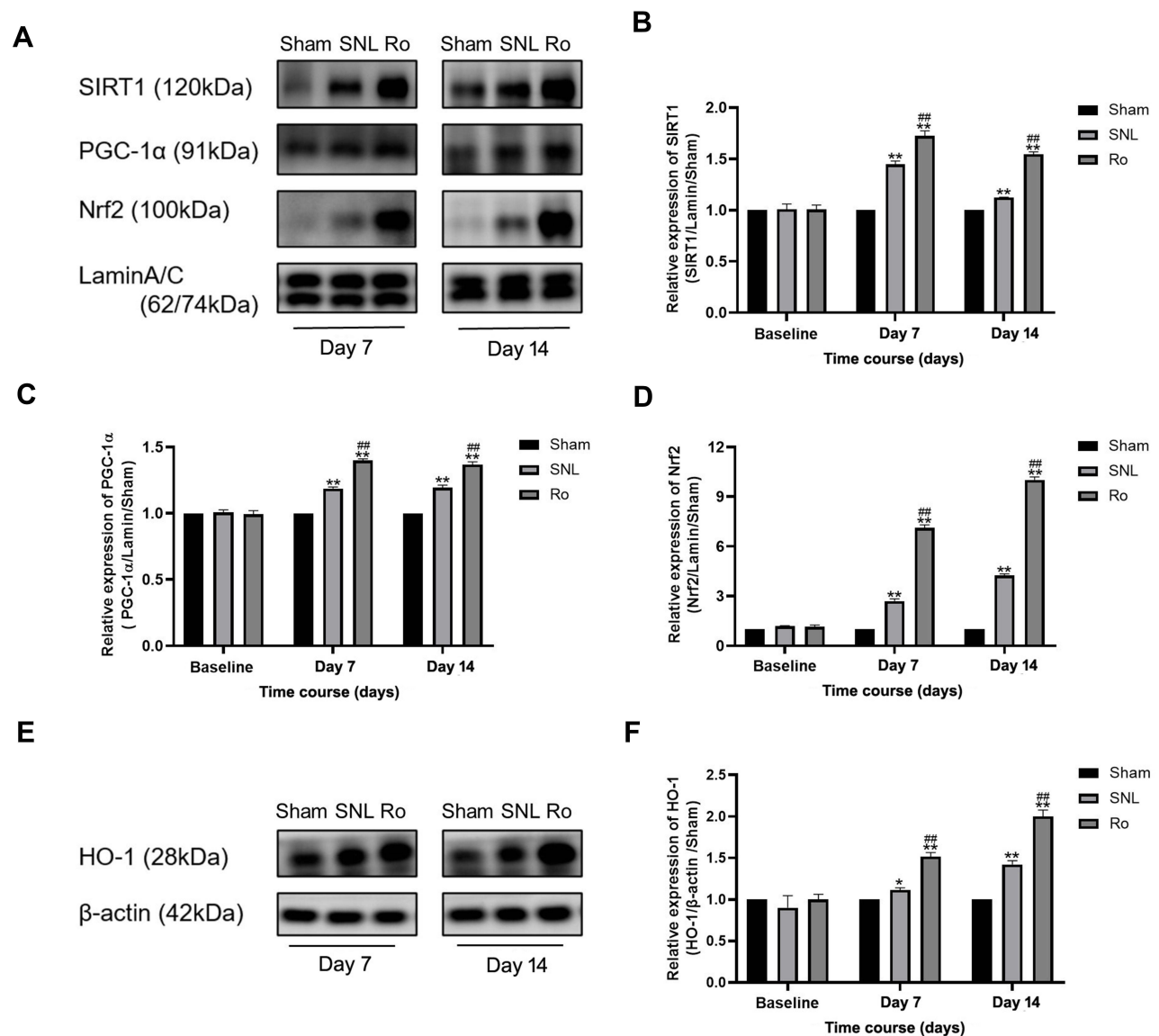


Figure 6 Effects of TSPO agonist Ro5-4864 on nuclear SIRT1/PGC-1 α signaling. (A) Representative immunoblots for nuclear SIRT1, PGC-1 α and Nrf2 contents of the Sham group, SNL group and Ro group on Day 7 and Day 14. (B–D) Illustration of the relative expression of nuclear SIRT1/lamin/Sham (B) PGC-1 α /lamin/Sham (C) and Nrf2/lamin/Sham (D) of the Sham group, SNL group and Ro group. * $P < 0.05$ and ** $P < 0.01$ compared with the Sham group at the same point in time. *** $P < 0.001$ compared with the SNL (control) group at the same point in time. (E) Representative immunoblots for cytoplasmic HO-1 contents of the Sham group, SNL group and Ro group on Day 7 and Day 14. (F) Illustration of the relative expression of cytoplasmic HO-1/ β -actin/Sham. * $P < 0.05$ and ** $P < 0.01$ compared with the Sham group at the same point in time. *** $P < 0.001$ compared with the SNL (control) group at the same point in time. $n = 4$ for each point of time in each group.

Discussion

In this study, we reported that TSPO agonist alleviated the allodynia induced by SNL, which was totally abrogated by autophagy inhibitor 3-MA. SNL induced spinal autophagic flux but an impaired autophagic degradation, demonstrated by elevated ATG7, Beclin1, and LC3-II/LC3-I and p62 accumulation. TSPO agonist Ro5-4864 augmented autophagy and improved autophagosome degradation compared with the SNL group. This autophagy promotion effect of Ro5-4864 could also be abrogated by 3-MA. Furthermore, Ro5-4864 activated the spinal nuclear SIRT1/PGC-1 α signaling pathway, which has been demonstrated to be antioxidant and cytoprotective in both autophagy and NP.

Initially, TSPO expression in the brain was considered to be specific for activated microglia thereby representing an inflammation biomarker.^{19,20} Many recent studies demonstrated TSPO agonists to be effective and protective in treatment of many neurological and psychiatric disorders including the neuropathic pain.^{14,19–21} In this present study, we found that

2 μ g of intrathecal Ro5-4864 repeated for three days could provide remarkable analgesic effect against the neuropathic pain induced by SNL, which was in accordance with our previous study.¹⁴ Moreover, we first reported that this analgesic effect of Ro5-4864 could be totally abrogated by autophagy inhibitor 3-MA, which suggested that autophagy may play a vital role in TSPO's protective effects.

Although the precise mechanisms remain unclear, there are several possible explanations for the analgesic effects of TSPO. First, we demonstrated that TSPO could improve the impaired autophagy induced by NP. One of the key steps in autophagy regulation is the phosphatidylethanolamine conjugation to the LC3-I to form lipidated LC3-II. This conjugation is regulated by some autophagy-related genes such as ATG7. Beclin1 complex is involved in autophagosome formation at an early stage and is essential for the recruitment of other autophagy-related proteins to the pre-autophagosomal structure.^{18,22} However, LC3-II upregulation will be associated with P62 accumulation, if this autophagy substrate is not been efficiently degraded. P62 is considered a useful readout of the final degradative steps of autophagy.²³ Our results showed that SNL induced a significant increase in ATG7, Beclin1, and LC3-II/LC3-I with elevated p62 content, which indicated an increased autophagic flux but a defective autophagosome clearance. Ro5-4864 elicited more activated ATG7, Beclin1 and LC3-II/LC3-I expression associated with decreased P62 compared with the SNL group, which indicated a more activated autophagic state and a more fluent autophagic process. These effects of Ro were totally abrogated by autophagy inhibitor 3-MA. The ultrastructure results are also in accordance with the Western blot results.

Second, accumulating evidence has indicated that oxidative stress and mitochondrial dysfunction are involved in chronic pain.^{24,25} Mitochondrial biogenesis is the process which restores mitochondrial against injuries.^{26,27} PGC-1 α and Nrf2 are two master regulators of endogenous antioxidant defense and mitochondrial biogenesis.^{28,29} Mitochondrial biogenesis process is initiated by the activation of PGC-1 α either by deacetylation (via SIRT1) or phosphorylation. PGC-1 α activation can perform transcriptional coactivation on the Nrf (The nuclear transcription factor) transcriptional (eg: Nrf2) activators to stimulate gene expression of mitochondrial genes.²⁶ Activation of SIRT1/PGC-1 α has been illustrated to alleviate neuropathic pain induced by type 2 diabetes²⁸ or chronic constriction injury (CCI) in the spinal cord and dorsal root ganglion.²⁹ Under oxidative stress conditions, Nrf2 translocates to the nucleus to activate gene expression of Phase II cytoprotective enzymes, which can exert cyto-protection or detoxify effects.^{30,31} Heme oxygenase (HO)-1 is a typical downstream phase II cytoprotective enzyme. Our previous study also demonstrated that HO-1 upregulation elicited potent analgesic effects against neuropathic pain.³² Therefore, we studied the effects of TSPO agonist Ro5-4864 on nuclear SIRT1/PGC-1 α pathway. We found that Ro5-4864 not only activated the nuclear SIRT1/PGC-1 α /Nrf2 pathway, but also upregulated cytoplasmic HO-1 expression compared with the SNL group. TSPO agonist provided both PGC-1 α and Nrf2 activation and downstream HO-1 elevation, thus improving mitochondrial biogenesis and NP plausibly. Furthermore, Nrf2 is not only downstream of PGC-1 α . They can form a feedback loop to elicit a more powerful effect.^{30,31}

Finally, a previous study of Li demonstrated that synergistic activation of both autophagy and the Nrf2 pathway had stronger analgesic effects than activation of autophagy alone.⁶ Our results showed that TSPO agonist can both activate the autophagy and Nrf2/HO-1 pathway. All these may offer several possible explanations for the potent analgesic and cytoprotective effects of TSPO.

There are some limitations in our present study. First, we previously reported that TSPO was mainly colocalized in astrocytes and partly colocalized in neurons in the spinal DH. Therefore, the elevation of autophagic proteins may be caused by both spinal astrocytes and neurons in DH. We did not measure these autophagic proteins in different types of cells separately. Li found that impaired autophagy of astrocytes could increase ROS levels and decrease glutathione in neurons co-cultured with them during oxidative stress.⁶ Therefore, indirect cooperation with neurons to affect the autophagy by TSPO in NP state could also not be excluded. Second, although we studied some mitochondrial biogenesis marker (eg, PGC-1 α and Nrf2), we did not investigate mitophagy directly. However, there have already been several studies that reported TSPO can improve mitophagy under various pathological conditions.^{15,16} Further in vitro studies using purified astrocytes are needed to elucidate these questions.

Actually, TSPO agonists were verified to provide an important protective role in a variety of diseases, such as ischemia, inflammation, anxiety and depression, neurotoxicity, oxidative stress, neuro-degenerative disease, even in some clinical trials. We hope that further studies on TSPO will provide a new strategy for treating NP.

Conclusion

In conclusion, TSPO agonist Ro5-4864 alleviated the allodynia induced by SNL, which was totally abrogated by autophagy inhibitor 3-MA. Ro5-4864 augmented autophagy and improved spinal autophagic flux compared with the SNL group. Furthermore, Ro5-4864 activated the spinal nuclear SIRT1/PGC-1 α signaling pathway and downstream Nrf2 and HO-1 expression, which has been demonstrated to be antioxidant and cytoprotective in both autophagy and NP.

Funding

This work was financial supported by National Nature Science Foundation of China (Grant Number 81771184).

Disclosure

Can Hao and Bingjie Ma are co-first authors for this study. The authors report no conflicts of interest in this work.

References

- Levine B, Klionsky DJ. Development by self-digestion: molecular mechanisms and biological functions of autophagy. *Dev Cell*. 2004;6(4):463–477. doi:10.1016/S1534-5807(04)00099-1
- Vigen RA, Kodama Y, Viset T, et al. Immunohistochemical evidence for an impairment of autophagy in tumorigenesis of gastric carcinoids and adenocarcinomas in rodent models and patients. *Histol Histopathol*. 2013;28(4):531–542. doi:10.14670/HH-28.531
- Cho K, Kim S, Choi SH. Suppressor of cytokine signaling 2 is induced in Huntington's disease and involved in autophagy. *Biochem Biophys Res Commun*. 2021;559:21–27. doi:10.1016/j.bbrc.2021.04.089
- Marcelo A, Afonso IT, Afonso-Reis R, et al. Autophagy in Spinocerebellar ataxia type 2, a dysregulated pathway, and a target for therapy. *Cell Death Dis*. 2021;12(12):1117. doi:10.1038/s41419-021-04404-1
- Berliocchi L, Maiarù M, Varano GP, et al. Spinal autophagy is differently modulated in distinct mouse models of neuropathic pain. *Mol Pain*. 2015;11:3. doi:10.1186/1744-8069-11-3
- Li J, Tian M, Hua T, et al. Combination of autophagy and NFE2L2/NRF2 activation as a treatment approach for neuropathic pain. *Autophagy*. 2021;17(12):4062–4082. doi:10.1080/15548627.2021.1900498
- Jin GL, Yue RC, He SD, Hong LM, Xu Y, Yu CX. Koumine decreases astrocyte-mediated neuroinflammation and enhances autophagy, contributing to neuropathic pain from chronic constriction injury in rats. *Front Pharmacol*. 2018;9:989. doi:10.3389/fphar.2018.00989
- Kang C, Li JL. Role of PGC-1 α signaling in skeletal muscle health and disease. *Ann NY Acad Sci*. 2012;1271(1):110–117. doi:10.1111/j.1749-6632.2012.06738.x
- Palikaras K, Tavernarakis N. Mitochondrial homeostasis: the interplay between mitophagy and mitochondrial biogenesis. *Exp Gerontol*. 2014;56:182–188. doi:10.1016/j.exger.2014.01.021
- Zhang T, Chi Y, Kang Y, et al. Resveratrol ameliorates podocyte damage in diabetic mice via SIRT1/PGC-1 α mediated attenuation of mitochondrial oxidative stress. *J Cell Physiol*. 2019;234(4):5033–5043. doi:10.1002/jcp.27306
- Guo X, Jiang Q, Tuccitto A, et al. The AMPK-PGC-1 α signaling axis regulates the astrocyte glutathione system to protect against oxidative and metabolic injury. *Neurobiol Dis*. 2018;113:59–69. doi:10.1016/j.nbd.2018.02.004
- Zehnder T, Petrelli F, Romanos J, et al. Mitochondrial biogenesis in developing astrocytes regulates astrocyte maturation and synapse formation. *Cell Rep*. 2021;35(2):108952. doi:10.1016/j.celrep.2021.108952
- Scarf AM, Ittner LM, Kassiou M. The translocator protein (18 kDa): central nervous system disease and drug design. *J Med Chem*. 2009;52(3):581–592. doi:10.1021/jm8011678
- Liu X, Liu H, Xu S, et al. Spinal translocator protein alleviates chronic neuropathic pain behavior and modulates spinal astrocyte-neuronal function in rats with L5 spinal nerve ligation model. *Pain*. 2016;157(1):103–116. doi:10.1097/j.pain.0000000000000339
- Frison M, Faccenda D, Abeti R, et al. The translocator protein (TSPO) is prodromal to mitophagy loss in neurotoxicity. *Mol Psychiatry*. 2021;26(7):2721–2739. doi:10.1038/s41380-021-01050-z
- Moras M, Hattab C, Gonzalez-Menendez P, et al. Downregulation of mitochondrial TSPO inhibits mitophagy and reduces enucleation during human terminal erythropoiesis. *Int J Mol Sci*. 2020;21(23):23. doi:10.3390/ijms21239066
- Chaplan SR, Bach FW, Pogrel JW, Chung JM, Yaksh TL. Quantitative assessment of tactile allodynia in the rat paw. *J Neurosci Methods*. 1994;53(1):55–63. doi:10.1016/0165-0270(94)90144-9
- Singh R, Cuervo AM. Lipophagy: connecting autophagy and lipid metabolism. *Int J Cell Biol*. 2012;2012:282041. doi:10.1155/2012/282041
- Chen MK, Guilarte TR. Translocator protein 18 kDa (TSPO): molecular sensor of brain injury and repair. *Pharmacol Ther*. 2008;118(1):1–17. doi:10.1016/j.pharmthera.2007.12.004
- Cosenza-Nashat M, Zhao ML, Suh HS, et al. Expression of the translocator protein of 18 kDa by microglia, macrophages and astrocytes based on immunohistochemical localization in abnormal human brain. *Neuropathol Appl Neurobiol*. 2009;35(3):306–328. doi:10.1111/j.1365-2990.2008.01006.x
- Chelli B, Pini S, Abelli M, et al. Platelet 18 kDa translocator protein density is reduced in depressed patients with adult separation anxiety. *Eur neuropsychopharmacol*. 2008;18(4):249–254. doi:10.1016/j.euroneuro.2007.10.003
- Cao L, Walker MP, Vaidya NK, Fu M, Kumar S, Kumar A. Cocaine-mediated autophagy in astrocytes involves sigma 1 receptor, PI3K, mTOR, Atg5/7, Beclin-1 and induces type II programmed cell death. *Mol Neurobiol*. 2016;53(7):4417–4430. doi:10.1007/s12035-015-9377-x
- Klionsky DJ, Abdalla FC, Abeliovich H, et al. Guidelines for the use and interpretation of assays for monitoring autophagy. *Autophagy*. 2012;8(4):445–544. doi:10.4161/auto.19496

24. Yamashita A, Matsuoka Y, Matsuda M, Kawai K, Sawa T, Amaya F. Dysregulation of p53 and parkin induce mitochondrial dysfunction and leads to the diabetic neuropathic pain. *Neuroscience*. 2019;416:9–19. doi:10.1016/j.neuroscience.2019.07.045
25. Canta A, Pozzi E, Carozzi VA. Mitochondrial dysfunction in Chemotherapy-Induced Peripheral Neuropathy (CIPN). *Toxics*. 2015;3(2):198–223. doi:10.3390/toxics3020198
26. Funk JA, Schnellmann RG. Accelerated recovery of renal mitochondrial and tubule homeostasis with SIRT1/PGC-1 α activation following ischemia-reperfusion injury. *Toxicol Appl Pharmacol*. 2013;273(2):345–354. doi:10.1016/j.taap.2013.09.026
27. Bernard K, Logsdon NJ, Miguel V, et al. NADPH oxidase 4 (Nox4) suppresses mitochondrial biogenesis and bioenergetics in lung fibroblasts via a Nuclear Factor Erythroid-derived 2-like 2 (Nrf2)-dependent pathway. *J Biol Chem*. 2017;292(7):3029–3038. doi:10.1074/jbc.M116.752261
28. Zhou CH, Zhang MX, Zhou SS, et al. SIRT1 attenuates neuropathic pain by epigenetic regulation of mGluR1/5 expressions in type 2 diabetic rats. *Pain*. 2017;158(1):130–139. doi:10.1097/j.pain.0000000000000739
29. Li X, Yang S, Wang L, et al. Resveratrol inhibits paclitaxel-induced neuropathic pain by the activation of PI3K/Akt and SIRT1/PGC1 α pathway. *J Pain Res*. 2019;12:879–890. doi:10.2147/JPR.S185873
30. Bellezza I, Giambanco I, Minelli A, Donato R. Nrf2-Keap1 signaling in oxidative and reductive stress. *Biochim Biophys Acta Mol Cell Res*. 2018;1865(5):721–733. doi:10.1016/j.bbamcr.2018.02.010
31. Baird L, Yamamoto M. The molecular mechanisms regulating the KEAP1-NRF2 pathway. *Mol Cell Biol*. 2020;40(13):13. doi:10.1128/MCB.00099-20
32. Liu X, Zhang Z, Cheng Z, et al. Spinal Heme Oxygenase-1 (HO-1) exerts antinociceptive effects against neuropathic pain in a mouse model of L5 spinal nerve ligation. *Pain Med*. 2016;17(2):220–229. doi:10.1111/pme.12906

Journal of Pain Research

Dovepress

Publish your work in this journal

The Journal of Pain Research is an international, peer reviewed, open access, online journal that welcomes laboratory and clinical findings in the fields of pain research and the prevention and management of pain. Original research, reviews, symposium reports, hypothesis formation and commentaries are all considered for publication. The manuscript management system is completely online and includes a very quick and fair peer-review system, which is all easy to use. Visit <http://www.dovepress.com/testimonials.php> to read real quotes from published authors.

Submit your manuscript here: <https://www.dovepress.com/journal-of-pain-research-journal>